

Effects of Interannual Salinity Variability on the Barrier Layer in the Western-Central Equatorial Pacific: A Diagnostic Analysis from Argo

ZHENG Fei^{*1}, ZHANG Rong-Hua^{2,3}, and ZHU Jiang¹

¹*International Center for Climate and Environment Science, Institute of Atmospheric Physics, Chinese Academy of Sciences, Beijing 100029*

²*Key Laboratory of Ocean Circulation and Waves, Institute of Oceanology, Chinese Academy of Sciences, Qingdao 266071*

³*Earth System Science Interdisciplinary Center, University of Maryland, College Park, Maryland 20740, USA*

(Received 26 April 2013; revised 24 July 2013; accepted 4 September 2013)

ABSTRACT

In this paper, interannual variations in the barrier layer thickness (BLT) are analyzed using Argo three-dimensional temperature and salinity data, with a focus on the effects of interannually varying salinity on the evolution of the El Niño–Southern Oscillation (ENSO). The interannually varying BLT exhibits a zonal seesaw pattern across the equatorial Pacific during ENSO cycles. This phenomenon has been attributed to two different physical processes. During El Niño (La Niña), the barrier layer (BL) is anomalously thin (thick) west of about 160°E, and thick (thin) to the east. In the western equatorial Pacific (the western part: 130°–160°E), interannual variations of the BLT indicate a lead of one year relative to those of the ENSO onset. The interannual variations of the BLT can be largely attributed to the interannual temperature variability, through its dominant effect on the isothermal layer depth (ILD). However, in the central equatorial Pacific (the eastern part: 160°E–170°W), interannual variations of the BL almost synchronously vary with ENSO, with a lead of about two months relative to those of the local SST. In this region, the interannual variations of the BL are significantly affected by the interannually varying salinity, mainly through its modulation effect on the mixed layer depth (MLD). As evaluated by a one-dimensional boundary layer ocean model, the BL around the dateline induced by interannual salinity anomalies can significantly affect the temperature fields in the upper ocean, indicating a positive feedback that acts to enhance ENSO.

Key words: barrier layer, salinity effect, ENSO, Argo

Citation: Zheng, F., R.-H. Zhang, and J. Zhu, 2014: Effects of interannual salinity variability on the barrier layer in the western-central equatorial Pacific: A diagnostic analysis from Argo. *Adv. Atmos. Sci.*, **31**(3), 532–542, doi: 10.1007/s00376-013-3061-8.

1. Introduction

Understanding the variations in the properties of the El Niño–Southern Oscillation (ENSO) has been a long-standing issue. The effects of salinity and its directly related atmospheric freshwater flux (FWF) forcing have been receiving more attention recently, because some related observations have become obtainable and these have shown that the relevant physical processes in the tropical Pacific have more important implications for ENSO variability (e.g., Delcroix et al., 2007; Cravatte et al., 2009; Zhang et al., 2010; Fujii et al., 2012; Zhang et al., 2012). Indeed, through their influences on the horizontal pressure gradients, equatorial thermocline, and vertical stratification, the FWF forcing and its related interannually varying salinity can have a significant effect on modulating the evolution of ENSO and tropical climate dynamics (e.g., Delcroix and Hémin, 1991; Murtugudde

and Busalacchi, 1998; Maes, 2000; Maes et al., 2002; Fedorov et al., 2004; Huang and Mehta, 2005). More recently, Zhang and Busalacchi (2009), and Zheng and Zhang (2012) demonstrated that salinity and its related FWF forcing can induce a positive feedback effect on the interannual variability associated with ENSO, through the stratification stability in the upper ocean. Another way in which FWF and salinity can affect the ocean is through the barrier layer (BL; Lukas and Lindstrom, 1991).

The BL has been known to be an important factor in initiating the onset of El Niño, as it has significant dynamic and thermodynamic consequences in the tropical Pacific. The BL can reduce or cut off the subsurface entrainment cooling into the mixed layer (ML) to isolate the warmer water of the upper layers (Lukas and Lindstrom, 1991; Maes et al., 2002), and enhance the warm pool displacements through restricting the response to the atmospheric wind forcing in a shallower ML (Maes et al., 1997; Vialard and Delecluse, 1998a, 1998b; Vialard et al., 2002). Lukas and Lindstrom (1991) first reported the existence of the BL in the western tropical Pacific

* Corresponding author: ZHENG Fei
Email: zhengfei@mail.iap.ac.cn

because of the salinity stratification, and increased attention has been paid to the salinity-induced BL processes in recent years, since its variability is intrinsically linked to ENSO dynamics (e.g., Picaut et al., 1996; Ando and McPhaden, 1997; Maes, 2000; Delcroix and McPhaden, 2002; Maes et al., 2002). However, most of these studies were limited due to a rather poor spatial/temporal data resolution for computing the barrier layer thickness (BLT; Bosc et al., 2009; Fujii et al., 2012). As salinity stratification is fundamental for the BL formation, it is necessary to quantify the role that salinity plays in the interannual variability of the BL.

However, the variations of the BL in the tropical Pacific have only been verified by a few studies because performing such work needs long-term concurrent temperature and salinity observations with adequate vertical resolution (e.g., Bosc et al., 2009). Thus, a unique opportunity exists now to make a more comprehensive analysis of the BL variability related to other atmospheric/oceanic states, since unprecedented three-dimensional temperature and salinity data have become obtainable from Argo observations (e.g., Sato et al., 2004; Maes et al., 2005; Sato et al., 2006; Maes, 2008; Bosc et al., 2009). More recently, using direct Argo data and some diagnostic fields, Zheng and Zhang (2012) found that the ENSO-induced salinity anomaly is a significant factor in modulating the variations of the ML in the western-central equatorial Pacific, which contributes to further enhancing the ENSO cycle in two ways. The effects of the salinity variability on the BL in this region are suspected to be important for ENSO developments through BL processes, and further studies should be performed to quantify the role of the BL in the evolution of ENSO (e.g., Bosc et al., 2009).

In this work, we investigated the effects induced by salinity and FWF forcing with a focus on the BL. Based on the Argo data from 2005 to 2012, a novel diagnostic method was used to isolate the respective contributions of the interannually varying temperature and salinity to interannual variations in the BLT. This method can clearly illustrate the relative effects of interannual variations in temperature and salinity on oceanic fields (Zheng and Zhang, 2012). In particular, we analyzed the interannual BL variability in the western-central equatorial Pacific, where the interannual variability tends to be opposite to that in the western Pacific. Additionally, a one-dimensional boundary layer model was adopted to investigate the roles of the BL variability in the modulation of the SST in the western-central basin.

The rest of this paper is organized as follows. Section 2 briefly describes the oceanic observational data used, and the analysis method adopted to isolate the relative effects of interannually varying or climatological temperature and salinity fields on the BLT variations. Section 3 provides an overview of the interannual variability from observed oceanic fields and the derived BLT field. Section 4 is further concerned with the relative contributions of interannually varying temperature and salinity to the interannual variations in the BLT. In section 5, the roles of the BL variability induced by the interannual salinity anomaly in modulating the SST are investigated using a one-dimensional boundary layer model. Fi-

nally, a summary and conclusion are presented in section 6.

2. Dataset, analysis procedures, and 1-D boundary ocean model

2.1. Dataset

The three-dimensional gridded temperature and salinity data used in this paper are from the Argo products, and were provided by the International Pacific Research Center (IPRC)/Asia-Pacific Data-Research Center (APDRC). The dataset includes the monthly mean and climatological fields with a 1° horizontal resolution at the standard depths (Levitus, 1982). Monthly and climatological BLT data were also estimated and provided by the IPRC/APDRC. All these Argo-based data are from 2005 to 2012, and are available online at <http://apdrc.soest.hawaii.edu/projects/argo/>.

2.2. Analysis procedures

In this study, some additional oceanic fields, including the potential density, the mixed layer depth (MLD), the isothermal layer depth (ILD), and the BLT, were analyzed using the three-dimensional temperature and salinity data. Here, the technique adopted in de Boyer Montégut et al. (2004) and Bosc et al. (2009) was used for estimating the MLD, ILD, and BLT. We define the BLT as the difference between the MLD and the ILD when the MLD is shallower than the ILD, and the MLD (ILD) is calculated as the depth where the density (temperature) is $\Delta\rho$ higher (ΔT lower) than that at 10 m depth, where $\Delta T = 0.2^\circ\text{C}$ and $\Delta\rho = -(\partial\rho/\partial T)\Delta T$. The potential density (i.e., relative to the sea surface) was calculated using the standard routine in Gill (1982).

To isolate the temperature and salinity contributions, a diagnostic method was proposed by Zheng and Zhang (2012) to access the relative effects of climatological or interannually varying temperature and salinity fields on an interannual anomaly field [Table 1 in Zheng and Zhang (2012)]. Being dependent on T (temperature) and S (salinity), a field is denoted as $F(T, S)$, whose interannual anomaly can be attributed to that of temperature and/or salinity. In this paper, the three-dimensional temperature and salinity data are taken as being either climatological or interannually varying [Table 1 in Zheng and Zhang (2012)] to diagnostically calculate a related oceanic field, including the MLD, ILD, and BLT. Based on these diagnostic results, the contributions of interannual variations in temperature and/or salinity to those in F can be quantified.

2.3. A single-column ocean model

To qualitatively evaluate the BLT effects on the variations of the thermal state in the upper ocean, a one-dimensional water column boundary layer model was adopted that is based on the Mellor and Yamada level 2.5 (MY2.5 model hereafter) turbulence closure scheme (Mellor and Yamada, 1982), with modifications by Galperin et al. (1988) and the parameter adjusted by Kantha and Clayson (1994). The six-hourly forcing fields for the MY2.5 model include heat flux, momen-

tum flux, and FWF data, which are all from the NCEP/DOE AMIP-II Reanalysis (NCEP2; Kanamitsu et al., 2002); simulations with two 30-day periods were tested, one from 1–30 November 2009 for an El Niño event, and the other from 1–30 October 2010 for a La Niña event.

3. Overview of interannual variability from observed oceanic fields and derived BLT

3.1. Total fields

The interannual variations along the equator of the observed SST, sea surface salinity (SSS), and derived BLT from APDRC are shown in Fig. 1. In general, the SST had a large interannual variation in the eastern equatorial Pacific, where cool waters occur during fall and warm waters take their place in spring (Fig. 1a). Fresh waters were evident in the far western equatorial Pacific, denoted as the fresh pool, and saline waters were located in the central basin with a front near the dateline (Eldin et al., 1997), which is directly associated with a convergence of water masses (Fig. 1b; Picaut et al., 1996). Interannual variations in SST and SSS are associated with ENSO events, which are predominantly controlled by the air–sea interaction processes among winds, SST, and the thermocline (e.g., Zhang and Zebiak, 2004). Large longitudinal displacements of the cold tongue were evident in the eastern equatorial Pacific and those of the warm/fresh pool were clearly observed in the west (Fig. 1a). For example, dur-

ing the 2009/10 El Niño, the warm pool in the west extended eastward along the equator, and the cold tongue shrank in the east, with the 27°C isotherm of SST locating east of 130°W. During the 2007/08 La Niña, the warm waters retreated to the west, while the cold tongue area developed anomalously and was strong in the east and expanded westward along the equator, with the 26°C isotherm of SST locating west of 160°W. Along the equator, the SSS front also moved back and forth associated with ENSO events (Fig. 1b). For example, during the 2009/10 El Niño, an observed freshening occurred in the central basin, accompanied by the extension of the fresh pool eastward beyond the dateline.

The analyses of the TOPEX/Poseidon and *in situ* data can also be performed to show the coexistence of heat build-up and a significant BL in the western equatorial Pacific (e.g., Maes et al., 2002). The time–longitude variability of the BLT along the equator (Fig. 1c) was similar to the variability observed during previous ENSO events (e.g., McPhaden and Zhang, 2009). The BL was found to be an almost permanent and robust feature of the western Pacific (e.g., Maes, 2000), which extended into the central basin only when the El Niño occurred (i.e., 2006/07 and 2009/10 El Niño). As described in previous studies (e.g., Maes et al., 2002; Maes et al., 2006; Bosc et al., 2009), the region of the thick BL is strongly correlated with the zonal displacements of the SSS front and the warmest SST. Most of the time, the larger values of BLT (i.e., above 20 m) were confined to the eastern edge of the warm pool (i.e., identified by the isotherm 29.0°C, red line in Fig.

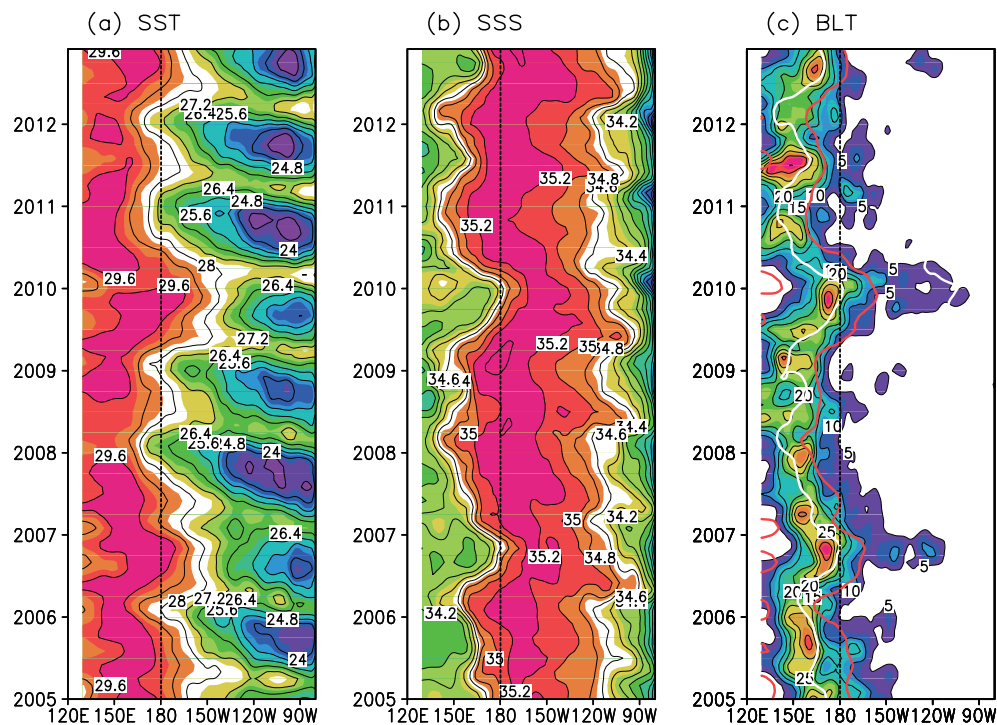


Fig. 1. Longitude–time sections along the Equator (averaged between 2°N and 2°S) for (a) SST, (b) SSS, and (c) derived BLT from the APDRC products during the 2005–12 period. The contour interval is 0.8°C in (a), 0.2 psu in (b), and 5.0 m in (c). The white line in (c) indicates the 34.6 isohaline serving as a position of the salinity front, and the red line in (c) denotes the 29.0°C isotherm.

1c), and the maximum values of BLT were located around the SSS front (i.e., marked by the 34.6 isohaline, white line in Fig. 1c), following its low frequency zonal displacement.

3.2. Anomaly fields

Figure 2 shows the interannual variations in various oceanic fields along the Equator. In terms of spatial structure, the SST had the largest variability (Fig. 2a) in the central and eastern equatorial Pacific, while large SSS anomalies (Fig. 2b) occurred in the western and central basin. The interannual variations in SSS showed a standing horizontal pattern concentrating in the western-central equatorial Pacific around the dateline, where the FWF also had a large variability (e.g., Zhang and Busalacchi, 2009). During El Niños, the anomalous SST was warm in the eastern and central basin and the anomalous SSS was low in the central and western basin. During the evolution into the La Niña phase, the anomalous SST was cold and the SSS became anomalously high in the central equatorial Pacific (e.g., Zheng and Zhang, 2012).

A distinct interannual variation of the BLT was seen in the equatorial Pacific Ocean (Fig. 2c). As noted by Maes (2000), variability in the BLT was different for the western part (i.e., western tropical Pacific; 130°E – 160°E) and eastern part (i.e., central tropical Pacific; 160°E – 170°W), a seesaw pattern of the interannual variations of the BLT was evident in the zonal direction (Fig. 2c). During El Niño (La Niña), the BL was anomalously thin (thick) west of about 160°E , and thick (thin) to the east.

In the western basin, a significant positive BLT anomaly

(i.e., a thicker BL than climatology) was seen prior to the 2006/07 and 2009/10 El Niño events (i.e., between mid-2005 and mid-2006, and from mid-2007 to mid-2009), which represents an essential condition for the sustained heat accumulation in the warm pool (e.g., Maes et al., 2005). The BLT was reduced, beginning in the west as the positive BLT anomalies (i.e., the maximum values of BLT) were displaced eastward in association with the onset of the two El Niño events (Fig. 2a). In the western basin, negative BLT anomalies were also observed before the onset of the 2007/08 and 2010/11 La Niña events, and the eastward spread of the negative BLT anomalies (i.e., a thinner BL than climatology) was observed during the development of the two La Niña events.

As shown in Fig. 3a, interannual variations in the BLT in the western equatorial Pacific and those in ENSO are out of phase; the lagged correlation indicates that the interannual changing of the BL in that region leads those of the Niño3.4 index by about twelve months. These phase relationships indicate that the interannual variations of the BLT in the western equatorial Pacific are about one-year ahead of ENSO (e.g., Maes et al., 2005), and demonstrate the importance of the BL in the western basin for the buildup of ENSO events. Moreover, the relative contributions of the MLD and ILLD to the BLT change are compared through calculating the regression coefficient between the interannual changes in the BLT and ILLD and between those in the BLT and MLD. In the western part (i.e., 130° – 160°E) for 2005 to 2012, the regression coefficients of the BLT with MLD/ILLD are 0.113/1.108, respectively. These analysis results indicate that the interan-

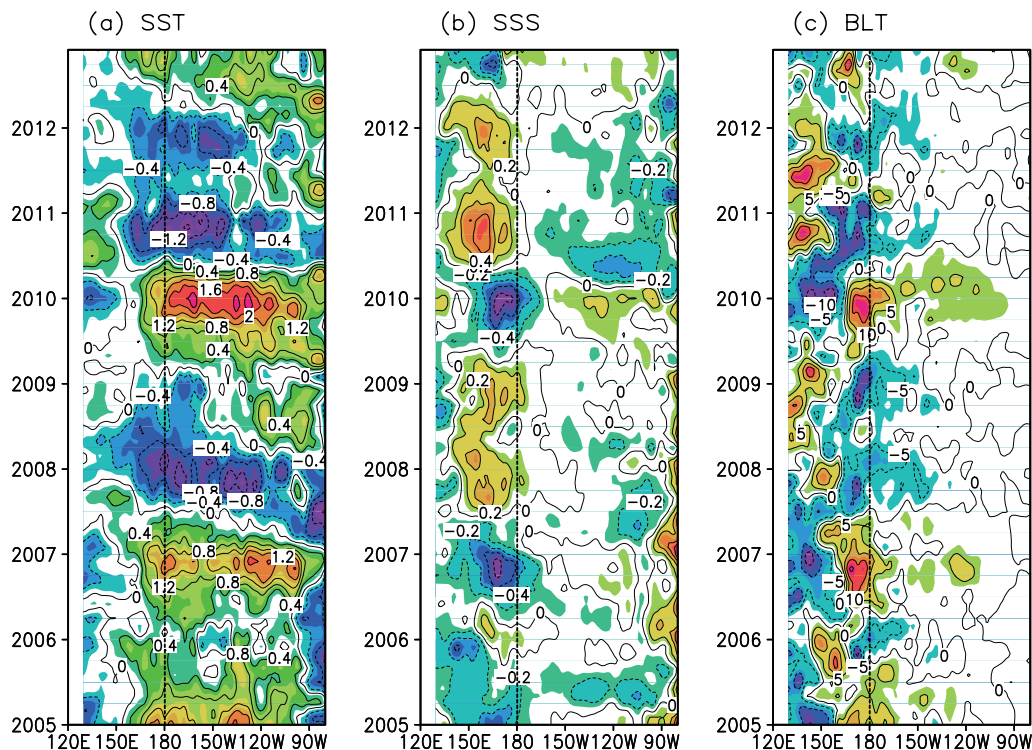


Fig. 2. The same as Fig. 1, except for the interannual anomalies of (a) SST ($^{\circ}\text{C}$), (b) SSS (psu), and (c) derived BLT (m). The contour interval is 0.4°C in (a), 0.2 psu in (b), and 5.0 m in (c).

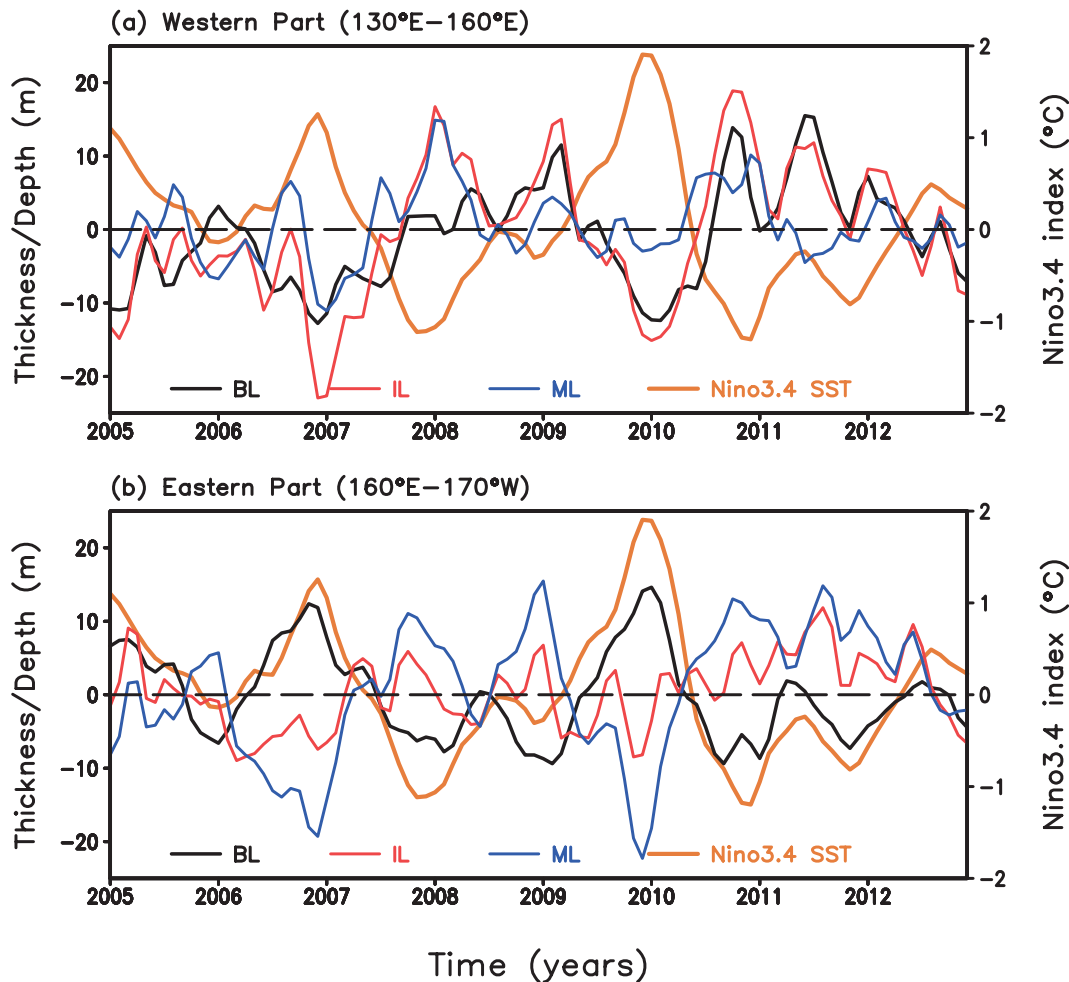


Fig. 3. Time series averaged in (a) the western part (2°S – 2°N , 130° – 160°E) and (b) the eastern part (2°S – 2°N , 160°E – 170°W) during 2005–12 for some derived fields from APDRC products: anomalous depth of ML (blue line); IL (red line); anomalous thickness of BL (black line); and Niño3.4 index (orange line).

nual changes of the BL in the western equatorial Pacific are, on average, primarily due to the interannual variations of the ILD and secondarily due to those of the MLD.

However, different from the leading effects of the BL in the western basin on the onset of ENSO events, the BL in the central basin (i.e., 160°E – 170°W) almost synchronously varied with ENSO (Fig. 3b). In this region, the BL became slightly thicker around the occurrences of the 2006/07 and 2009/10 El Niño events, presenting a significant effect of thick BLT on warming the ML and enhancing El Niño. However, a strong negative BLT anomaly was evident in the central equatorial Pacific during the 2007/08, 2008/09, and 2010/11 La Niña events; a relatively thin BL helps to enhance the development of the cold event through increasing the entrainment cooling from below the ML. Furthermore, in the eastern part (i.e., 160°E – 170°W) and for the entire period, the regression coefficients of the BLT with MLD/ILD were $-1.125/-0.121$, respectively (Fig. 3b). These analyses indicate that the interannual changes of the BL in the central equatorial Pacific are, on average, primarily due to the interannual variations of the MLD and secondarily due to those

of the ILD. The following sections focus on the interannual variations of the BLT in the central Pacific, which have not been explored as much in previous studies.

4. The salinity contributions to interannual BLT anomalies: a diagnostic analysis

As mentioned in the introduction, a BL can be created between the base of the ML and the bottom of the isothermal layer (IL) due to the action of salinity stratification, thus the variations in the BLT are controlled by both the variations in the MLD and in the ILD. As shown in Fig. 3, interannual variations of the BLT can be attributed to two different factors. In the western equatorial Pacific (western part: 130° – 160°E), interannual variations of the BLT are mainly attributed to the interannually varying ILD field. But in the central equatorial Pacific (eastern part: 160°E – 170°W), interannual variations of the BL are primarily affected by those of the ML.

Thus, the interannual variations in the BLT (i.e., the see-saw pattern shown in Fig. 2c) are not only related to those in

salinity but also to those in temperature. The approach proposed by Zheng and Zhang (2012) allows the investigation of the roles of temperature and salinity variability in the interannually varying BLT. In this section, four diagnostic calculations are made, in which the temperature and salinity fields used are either climatological or interannually varying [Table 1 in Zheng and Zhang (2012)].

The interannual variation of the BLT is also well presented by the diagnosed anomalous BLT as calculated from the interannual analysis, “ $BLT(T_{inter}, S_{inter}) - BLT(T_{clim}, S_{clim})$ ” (Fig. 4a; T_{inter} and S_{inter} represent interannually varying temperature and salinity fields, respectively; T_{clim} and S_{clim} represent climatological temperature and salinity fields, respectively), and the interannual BLT anomalies calculated in this way have a similar spatial–temporal pattern to those directly derived from APDRC products (Fig. 2c). The other two interannual analyses illustrate the relative effects of salinity and temperature on the BLT field [Fig. 4b: “ $BLT(T_{clim}, S_{inter}) - BLT(T_{clim}, S_{clim})$ ” and Fig. 4c: “ $BLT(T_{inter}, S_{clim}) - BLT(T_{clim}, S_{clim})$ ”], respectively. Around the dateline, a striking feature is that interannual anomalies of salinity make a significant contribution to the BLT variability, whereas those of temperature are the major contributor in the western basin through their dominant effect on the ILD (Fig. 3a). For example, the strong shoaling of the BL in the central basin during the 2010/11 La Niña was largely due to the effects of the positive salinity anomalies. Moreover, the effects diagnosed for

the relative contributions of interannually varying temperature and salinity to the BLT are not sensitive to the diagnostic method of the BLT adopted here. In fact, similar results can be obtained when the criterion is chosen as $\Delta T = 0.5^\circ\text{C}$ and the reference layer is the surface (e.g., Maes et al., 2005).

As the influences of the interannually varying salinity on BLT are mainly located in the central equatorial Pacific, Fig. 5 compares the interannual anomalies of the BLT in three different interannual analyses over the central equatorial region ($2^\circ\text{S} - 2^\circ\text{N}$, $170^\circ\text{E} - 170^\circ\text{W}$) for 2005 to 2012. The SST averaged in the central basin is also used as an indicator of the local SST variations in Fig. 5. A close relationship between the variations in BLT and SST is seen on the interannual time scale (Fig. 5), with their positive correlation (i.e., 0.76) in the central equatorial Pacific. Additionally, the lagged correlation indicates that the interannual variations of the BL in the central equatorial Pacific (i.e., black line in Fig. 5) lead those of the SST (i.e., gray line in Fig. 5) by about two months. This also means that the BL in the central basin could be regarded as a precursor of the local SST variation in the central tropical Pacific.

As the largest variability of salinity was around the eastern edge of the warm pool near the dateline, the significant effects of salinity on the vertical stratification were found to be a dominant factor affecting the MLD variability in the central basin (Zheng and Zhang, 2012). Thus, the effects of interannually varying salinity on the BLT were also sig-

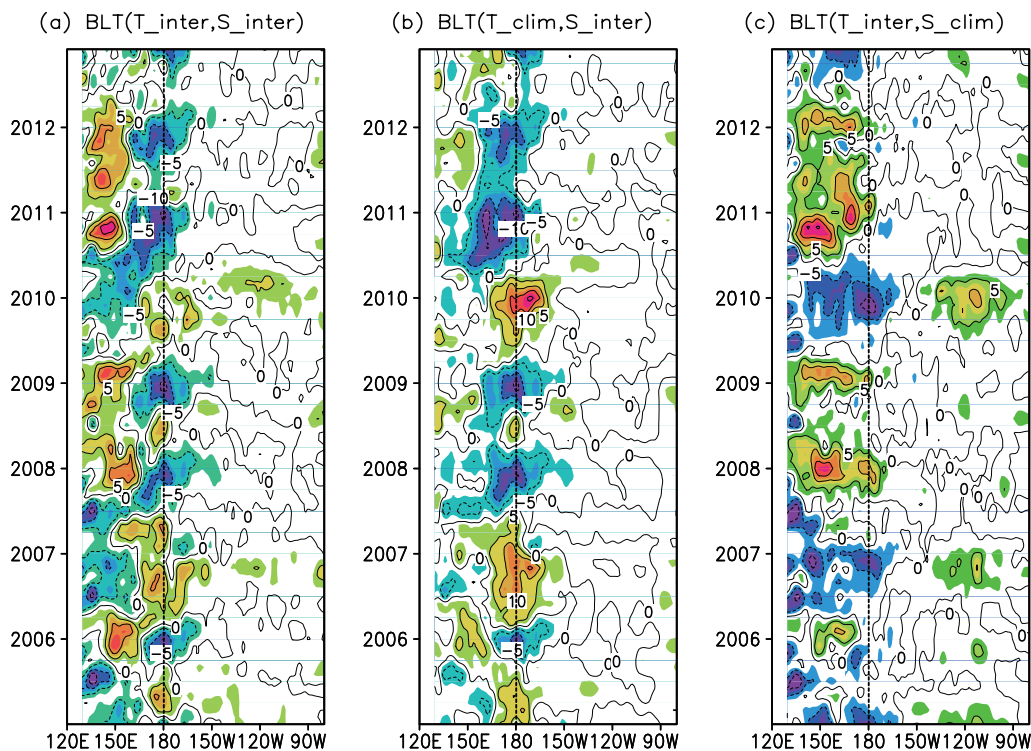


Fig. 4. Longitude–time sections along the Equator (averaged from 2°N to 2°S) for the diagnosed BLT from 2005 to 2012. Three interannual calculations were made for the BLT field using (a) $BLT(T_{inter}, S_{inter})$, (b) $BLT(T_{clim}, S_{inter})$, and (c) $BLT(T_{inter}, S_{clim})$, respectively, and all these three calculations for BLT were deducted from the climatological BLT field [i.e., $BLT(T_{clim}, S_{clim})$]. The contour interval is 5 m for BLT.

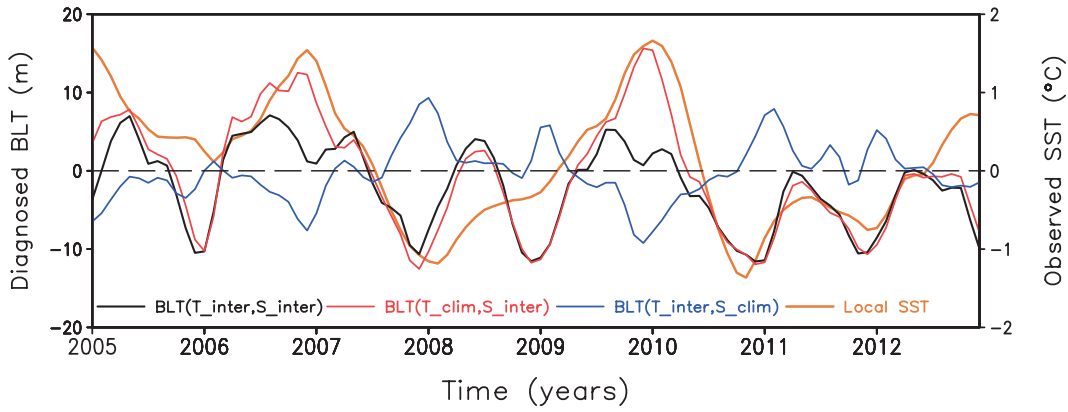


Fig. 5. Time series averaged in the central basin (2°S – 2°N , 170°E – 170°W) during 2005–12 for the three different interannual calculations of the interannually varying BLT, and the observed SST anomalies. Three calculations for BLT were all deducted from the climatological BLT field [i.e., $\text{BLT}(T_{\text{clim}}, S_{\text{clim}})$], allowing the examination of the relative contributions of salinity and temperature to the interannual variations of BLT.

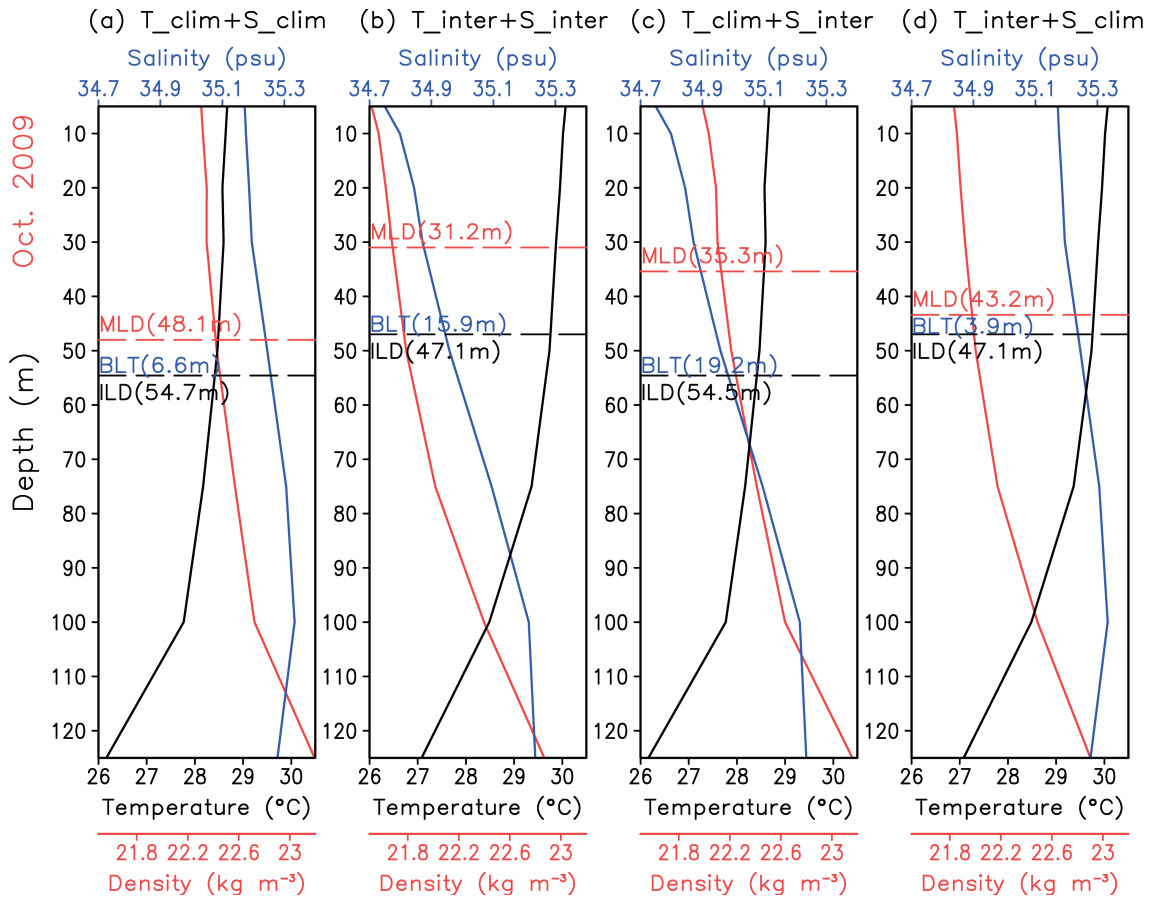


Fig. 6. Vertical profiles of density, temperature, salinity, and the associated MLD, ILD, and BLT in the central equatorial region [averaged in the area (2°S – 2°N , 175°E – 175°W)] for October 2009, representing an El Niño condition. Four different diagnostic methods are compared to illustrate the relative contributions of salinity and temperature to the variations of MLD, ILD, and BLT. The bottoms of ML and IL are denoted by the red and black dashed lines. Units are respectively in $^{\circ}\text{C}$ for temperature, psu for salinity, kg m^{-3} for density, and m for MLD, ILD, and BLT.

nificantly larger than those of the interannually varying temperature in this region, as compared in Figs. 6 and 7. The other two interannual analyses distinguish the relative contributions of temperature and salinity to the temporally vary-

ing BLT field in the central equatorial Pacific (Fig. 5). The anomalous SST over the central equatorial Pacific (i.e., gray line in Fig. 5) follows the BLT anomalies induced by interannually varying salinity (i.e., red line in Fig. 5) quite well,

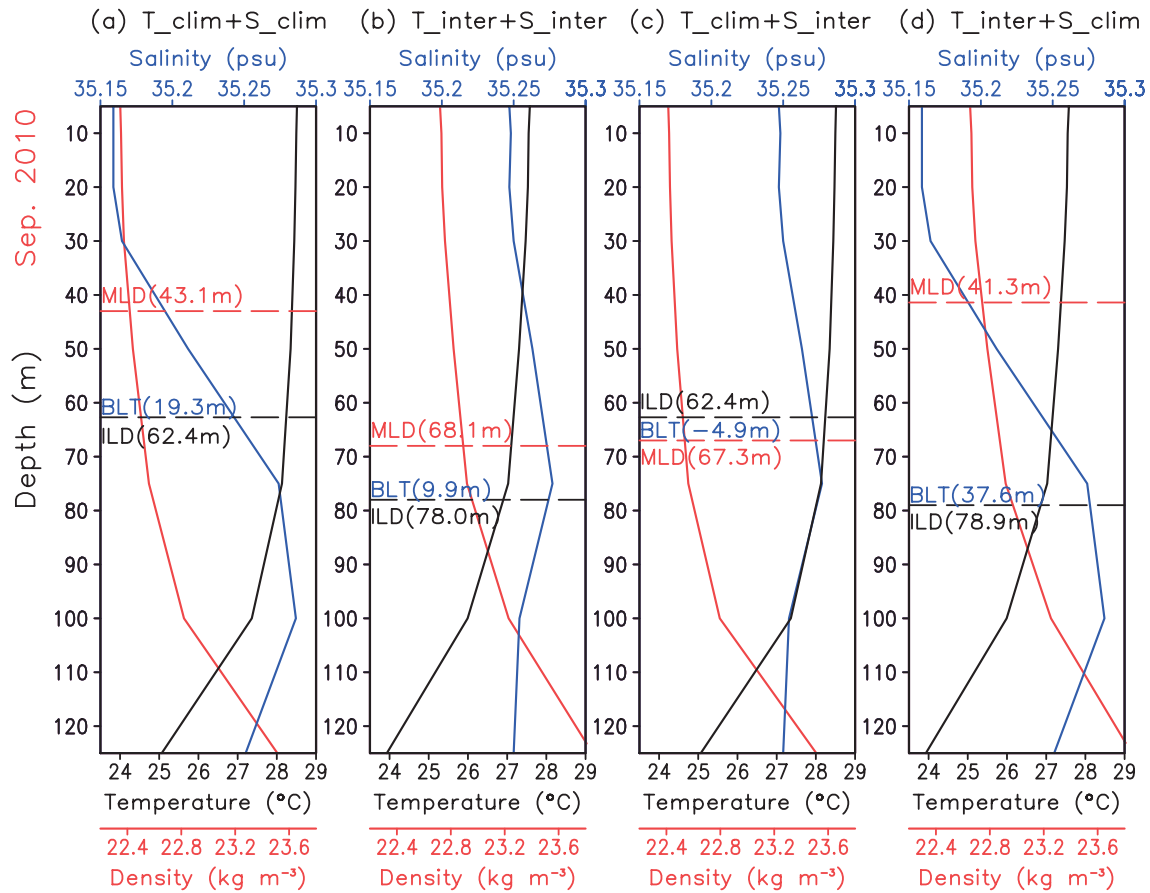


Fig. 7. The same as Fig. 6, except for a La Niña condition in September 2010.

and the lagged correlation was maximum (i.e., 0.86) when the anomalous BLT led the local SST anomalies by around two months. The BLT variability was further enhanced by the effects of the interannual salinity variations. For instance, a thicker BL was seen in October 2009 (i.e., BLT in Fig. 6c is 3.3 m thicker than that in Fig. 6b), and even a compensating layer was present in September 2010 (i.e., BLT in Fig. 7c is 14.8 m thinner than that in Fig. 7b); the two cases both potentially provide a more favorable condition for the development of ENSO events. However, the interannually varying temperature presents an opposite contribution to influencing the variations of BLT (i.e., green line in Fig. 5), which have a negative correlation (i.e., -0.66) with those of the local SST. For example, the BLT induced by the interannually varying temperature decreased to 3.9 m in October 2009 (Fig. 6d), and increased to 37.6 m in September 2010 (Fig. 7d), which acted to inhibit the development of the ENSO.

Comparisons among these analyses indicate that the effects of interannually varying salinity mainly contribute to the interannual variations in the BLT over the central equatorial Pacific through controlling those in the ML. The interannual salinity anomalies tend to enhance the interannual variability of the BL, which in turn affects the SST, and other atmospheric and oceanic fields are expected to exert a significant modulation on ENSO. Moreover, the interannually varying temperature field acts to decrease the BLT variability in this

region, and partially compensates for the salinity effects.

5. Salinity effects on BLT during ENSO evolutions: A 1-D model simulation

As described above, the main effect of the BL is to reduce or cut off the subsurface entrainment cooling into the ML to isolate the warmer water in the upper layers (Lukas and Lindstrom, 1991; Maes et al., 2002). The relationship between the existence of the BL and ENSO evolution during the occurrence of ENSO events appears to be inherent in the central equatorial Pacific. At the same time, this relationship is even enhanced by the BL variability when only considering the effects of the interannually varying salinity. However, whether or not the existence of a thicker (thinner) BL induced by the negative (positive) salinity anomalies can produce a favorable condition for the development of an El Niño (La Niña) event in the central equatorial Pacific, the possible mechanism for the importance of the BL in the central basin still needs to be further explored.

Through adopting the single-column MY2.5 model and the six-hourly NCEP2 atmospheric forcing fields, two sets of simulation experiments (i.e., the salinity-effect experiment and the reference experiment) were performed during two 30-day periods (i.e., November 2009 for the El Niño case and

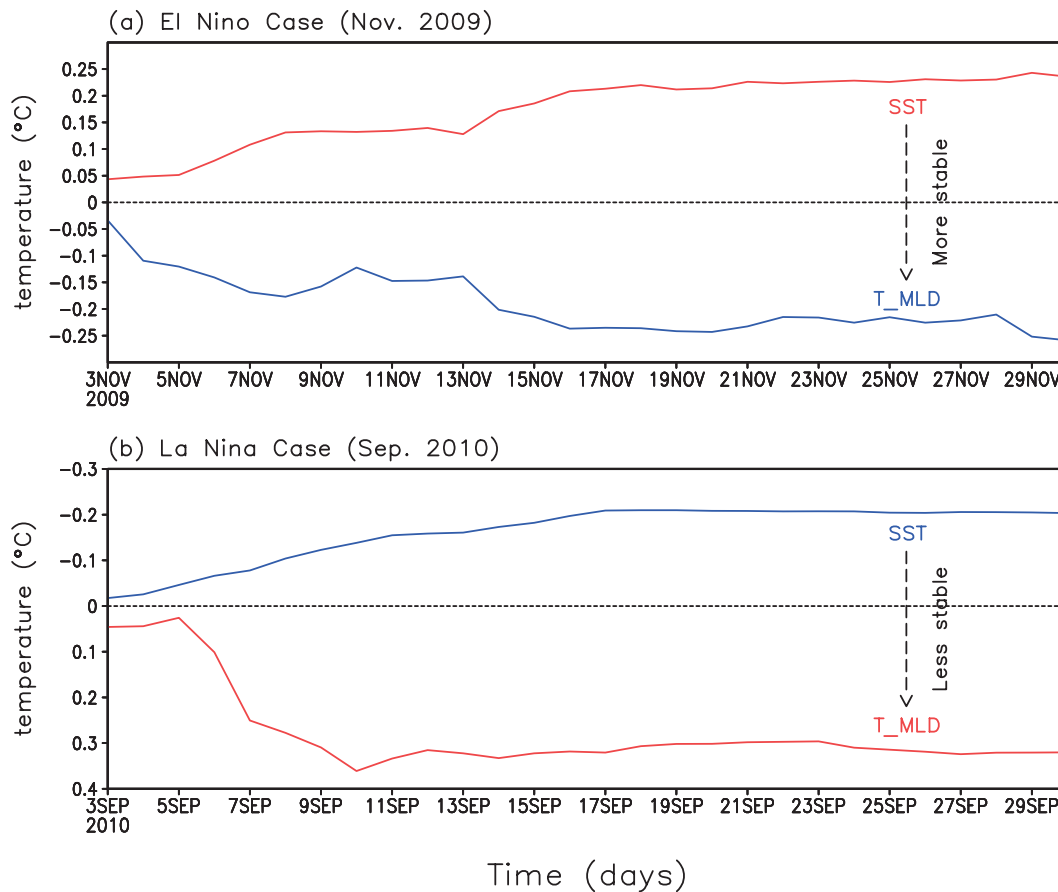


Fig. 8. Time series for the differences of SST and the temperature at the base of ML (T_{MLD}) between the salinity effect and the reference experiments [i.e., $TEMP(T_{inter}, S_{inter}) - TEMP(T_{inter}, S_{clim})$] in a 30-day integration for (a) an El Niño event during November 2009, and (b) a La Niña event during October 2010. To illustrate the effects of interannual salinity anomalies on the temperature changes in the upper ocean, two cases were tested: the salinity-effect experiment was initialized from interannually varying temperature and salinity profiles, and the reference experiment was initialized from the interannually varying temperature and climatological salinity profiles. The red line indicates a warming effect and the blue line indicates a cooling effect.

October 2010 for the La Niña case) to evaluate the potential effects of the BLT on the variations of the thermal state in the upper ocean. The MY2.5 model was set at a grid point in the central equatorial Pacific [i.e., (1.0°N, 180.0°W)], and the modeled water column was 1000 meters deep with a fixed 2-m vertical grid spacing. In the following, the salinity-effect experiment refers to a standard simulation initialized from both the interannually varying temperature and salinity profile, whereas the reference experiment was initialized from the interannually varying temperature and the climatological salinity profile. According to the experiment design, the difference between the salinity-effect experiment and the reference experiment was only from the initial salinity state. One is for the interannually varying salinity and the other is for the climatological salinity.

In November 2009, associated with the development of the 2009/10 El Niño event (figure not shown), a warmer SST and a colder temperature below the ML were simulated by the salinity-effect experiment (Fig. 8a), which mostly resulted from the initial negative salinity anomalies in the upper

ocean, through inducing a thicker BL at the initial time. All these can further lead to more stable stratification to reinforce the increment of the temperature in the ML. In October 2010, due to an initial thinner BL induced by the positive salinity anomalies, the absence of the BL led to a weaker heat build-up in the ML because of an expected increased entrainment cooling at its bottom. Less stable upper layers in the salinity-effect experiment were induced by the simulated colder SST and warmer temperature below the ML (Fig. 8b), which are favorable for developing a cold event.

6. Summary and conclusions

By isolating the ML from the entrainment of subsurface cold water, the BL can enhance the heat build-up and play an active role in the onset of El Niño. Early studies on the MLs neglected the role of salinity stratification due to the lack of salinity observations (Cooper, 1988). In this work, based on the unprecedented three-dimensional salinity and temperature data available from Argo, the interannual variability of

BL was investigated during 2005–12, which encompassed recent El Niño and La Niña events since 2005.

A BL exists in the tropical Pacific mainly because the top of the thermocline is deeper than that of the halocline. Thus, interannual variations in the BLT are controlled by the variations in the MLD and/or the ILD. In this work, we applied a novel diagnostic method to differentiate the relative contributions of interannually varying temperature and salinity fields to the interannually varying BL. A distinct interannual variation in the BLT over the equatorial Pacific Ocean is presented by the derived BLT anomalies (Fig. 2c). As noted by Maes (2000), variability in the BLT is different in the western part (i.e., western tropical Pacific) from the eastern part (i.e., central tropical Pacific), with a seesaw pattern of the interannual variations of BLT in the zonal direction. Similar to previous studies, the interannual variations of the BLT in the western Pacific were about one-year ahead of those of ENSO, indicating an essential circumstance for the heat build-up in the west, where the variability is controlled by the interannually varying temperature through its dominant effect on the isothermal layer depth (ILD).

Further, the diagnostic analyses in this work clearly demonstrate that the interannual variations in salinity, through dominantly affecting the ML variability, play a significant role in modulating the BL in the central basin, which also presents a precursor variation to the local SST. The enhanced interannual variability of the BL induced by interannual salinity anomalies in turn affects the temperature in the upper ocean, which serves as a positive feedback responsible for the development of ENSO events. Additionally, this finding is substantiated by the MY2.5 single column model in this work. During the development of an El Niño event, El Niño can induce a negative salinity anomaly in the western-central equatorial Pacific, which tends to decrease the oceanic density in the upper ocean, stabilize the upper layers, and reduce the MLD; then the thickness of the BL is increased and the entrainment of the subsurface cold water is reduced in turn. A warming effect on the SST with enhancing the El Niño development can be induced as the direct influence of these physical processes on isolating the subsurface entrainment into the ML and reducing the vertical mixing. How to enhance a La Niña event by a positive salinity anomaly and its related BLT variations through their modulation effects can be similarly quantified and illustrated accordingly.

Note that the salinity field itself does not play a direct role in air–sea interactions as it has no direct and immediate influence on the atmosphere. In this work, it was shown that the underlying climate feedback induced by the salinity effects can modulate ENSO through oceanic processes as explained above using Argo data and in Zheng and Zhang (2012). As in the ENSO theory described by Picaut et al. (1996), this work also confirmed that salinity stratification can play an important role in modulating SST evolution, which is included in the possible physical mechanisms of the positive feedback loop over the tropical Pacific. Here, the salinity-related effects are estimated on enhanced SST anomalies through modulating the interannual variations in the BLT over the central

equatorial Pacific, which are based on diagnostic analyses only.

These results support the view that the salinity variability can be a new contributor to ENSO variability. The large effects on ENSO demonstrated here also indicate a clear need to adequately take into account this mechanism in coupled ocean–atmosphere models, as the salinity effect has not been accurately included in most intermediated coupled models (ICMs; e.g., Zheng et al., 2006, 2007, 2009; Zheng and Zhu, 2010) used for ENSO simulation and prediction. Also, because this mechanism significantly modulates ENSO, misrepresentations of salinity-induced feedback are a clear source of model biases in the tropical Pacific. More coupled modeling studies are clearly needed to address these issues.

Acknowledgements. The authors wish to thank the two anonymous reviewers for their helpful comments. This research was supported by the National Basic Research Program of China (Grant No. 2012CB955202), and the National Natural Science Foundation of China (Grant No. 41176014).

REFERENCES

- Ando, K., and M. J. McPhaden, 1997: Variability of surface layer hydrography in the tropical Pacific Ocean. *J. Geophys. Res.*, **102**, 23 063–23 078.
- Bosc, C., T. Delcroix, and C. Maes, 2009: Barrier layer variability in the western Pacific warm pool from 2000 to 2007. *J. Geophys. Res.*, **114**, C06023, doi: 10.1029/2008JC005187.
- Cooper, N. S., 1988: The effect of salinity on tropical ocean models. *J. Phys. Oceanogr.*, **18**, 697–707.
- Cravatte, S., T. Delcroix, D. X. Zhang, M. McPhaden, and J. Leloup, 2009: Observed freshening and warming of the western Pacific warm pool. *Climate Dyn.*, **33**, 565–589, doi: 10.1007/s00382-009-0526-7.
- Delcroix, T., and C. Hénin, 1991: Seasonal and interannual variations of sea surface salinity in the tropical Pacific ocean. *J. Geophys. Res.*, **96**, 22 135–22 150.
- Delcroix, T., and M. McPhaden, 2002: Interannual sea surface salinity and temperature changes in the western Pacific warm pool during 1992–2000. *J. Geophys. Res.*, **107**(C12), doi: 10.1029/2001JC000862.
- Delcroix, T., S. Cravatte, and M. J. McPhaden, 2007: Decadal variations and trends in tropical Pacific sea surface salinity since 1970. *J. Geophys. Res.*, **112**, C03012, doi: 10.1029/2006JC003801.
- de Boyer Montégut, C., G. Madec, A. S. Fischer, A. Lazar, and D. Ludicone, 2004: Mixed layer depth over the global ocean: An examination of profile data and a profile-based climatology. *J. Geophys. Res.*, **109**, C12003, doi: 10.1029/2004JC002378.
- Eldin, G., M. Rodier, and M.-H. Radenac, 1997: Physical and nutrient variability in the upper equatorial Pacific associated with westerly wind forcing and wave activity in October 1994. *Deep-Sea Res. (II)*, **44**, 1783–1800.
- Fedorov, A.V., R. C. Pacanowski, S. G. Philander, and G. Boccaletti, 2004: The effect of salinity on the wind-driven circulation and the thermal structure of the upper ocean. *J. Phys. Oceanogr.*, **34**, 1949–1966.
- Fujii, Y., M. Kamachi, S. Matsumoto, and S. Ishizaki, 2012: Bar-

- rier layer and relevant variability of the salinity field in the equatorial Pacific estimated in an ocean reanalysis experiment. *Pure Appl. Geophys.*, **169**, 579–594.
- Galperin, B., L. H. Kantha, S. Hassid, and A. Rosati, 1988: A quasi-equilibrium turbulent energy model for geophysical flows. *J. Atmos. Sci.*, **45**, 55–62.
- Gill, A. E., 1982: *Atmosphere-Ocean Dynamics*. Academic Press, 662 pp.
- Huang, B. Y., and V. M. Mehta, 2005: Response of the Pacific and Atlantic oceans to interannual variations in net atmospheric freshwater. *J. Geophys. Res.*, **110**, C08008, doi: 10.1029/2004JC002830.
- Kanamitsu, M., W. Ebisuzaki, J. Woollen, S.-K. Yang, J. J. Hnilo, M. Fiorino, and G. L. Potter, 2002: NCEP-DOE AMIP-II reanalysis (R-2). *Bull. Amer. Meteor. Soc.*, **83**, 1631–1643.
- Kantha, L. H., and C. A. Clayson, 1994: An improved mixed layer model for geophysical applications. *J. Geophys. Res.*, **99**(C12), 25 235–25 266.
- Levitus, S., 1982: Climatological atlas of the world ocean. NOAA Professional Paper No. 13. US Government Printing Office, 173 pp.
- Lukas, R., and E. Lindstrom, 1991: The mixed layer of the western equatorial Pacific Ocean. *J. Geophys. Res.*, **96**, 3343–3357.
- Maes, C., 2000: Salinity variability in the equatorial Pacific Ocean during the 1993–98 period. *Geophys. Res. Lett.*, **27**, 1659–1662, doi: 10.1029/1999GL011261.
- Maes, C., 2008: On the ocean salinity stratification observed at the eastern edge of the equatorial Pacific warm pool. *J. Geophys. Res.*, **113**, C03027, doi: 10.1029/2007JC004297.
- Maes, C., P. Delecluse, and G. Madec, 1997: Impact of westerly wind bursts on the warm pool of the TOGA-COARE domain in an OGCM. *Climate Dyn.*, **14**, 55–70, doi: 10.1007/s003820050208.
- Maes, C., J. Picaut, and S. Belamari, 2002: Salinity barrier layer and onset of El Niño in a Pacific coupled model. *Geophys. Res. Lett.*, **29**(24), doi: 10.1029/2002GL016029.
- Maes, C., J. Picaut, and S. Belamari, 2005: Importance of salinity barrier layer for the buildup of El Niño. *J. Climate*, **18**, 104–118, doi: 10.1175/JCLI-3214.1.
- Maes, C., K. Ando, T. Delcroix, W. S. Kessler, M. J. McPhaden, and D. Roemmich, 2006: Observed correlation of surface salinity, temperature and barrier layer at the eastern edge of the western Pacific warm pool. *Geophys. Res. Lett.*, **33**, L06601, doi: 10.1029/2005GL024772.
- McPhaden, M. J., and X. B. Zhang, 2009: Asymmetry in zonal phase propagation of ENSO sea surface temperature anomalies. *Geophys. Res. Lett.*, **36**, L13703, doi: 10.1029/2009GL038774.
- Mellor, G. L., and T. Yamada, 1982: Development of a turbulence closure model for geophysical fluid problems. *Rev. Geophys.*, **20**(4), 851–875.
- Murtugudde, R., and A. J. Busalacchi, 1998: Salinity effects in a tropical ocean model. *J. Geophys. Res.*, **103**, 3283–3300.
- Picaut, J., M. Ioualalen, C. Menkes, T. Delcroix, and M. J. McPhaden, 1996: Mechanism of the zonal displacements of the Pacific warm pool: Implications for ENSO. *Science*, **274**, 1486–1489, doi: 10.1126/science.274.5292.1486.
- Sato, K., T. Suga, and K. Hanawa, 2004: Barrier layer in the North Pacific subtropical gyre. *Geophys. Res. Lett.*, **31**, L05301, doi: 10.1029/2003GL018590.
- Sato, K., T. Suga, and K. Hanawa, 2006: Barrier layers in the subtropical gyres of the world's oceans. *Geophys. Res. Lett.*, **33**, L08603, doi: 10.1029/2005GL025631.
- Vialard, J., and P. Delecluse, 1998a: An OGCM study for the TOGA decade. Part I: Role of salinity in the physics of the western Pacific fresh pool. *J. Phys. Oceanogr.*, **28**, 1071–1088.
- Vialard, J., and P. Delecluse, 1998b: An OGCM study for the TOGA decade. Part II: Barrier-layer formation and variability. *J. Phys. Oceanogr.*, **28**, 1089–1106.
- Vialard, J., P. Delecluse, and C. Menkes, 2002: A modeling study of salinity variability and its effects in the tropical Pacific Ocean during the 1993–1999 period. *J. Geophys. Res.*, **107**(C12), SRF6-1–SRF6-14, doi: 10.1029/2000JC000758.
- Zhang, R.-H., and S. E. Zebiak, 2004: An embedding method for improving interannual variability simulations in a hybrid coupled model of the tropical Pacific ocean-atmosphere system. *J. Climate*, **17**(14), 2794–2812.
- Zhang, R.-H., and A. J. Busalacchi, 2009: Freshwater flux (FWF)-induced oceanic feedback in a hybrid coupled model of the tropical Pacific. *J. Climate*, **22**, 853–879.
- Zhang, R.-H., G.-H. Wang, D. K. Chen, A. J. Busalacchi, and E. C. Hackert, 2010: Interannual biases induced by freshwater flux and coupled feedback in the tropical Pacific. *Mon. Wea. Rev.*, **138**, 1715–1737.
- Zhang, R.-H., F. Zheng, J. S. Zhu, Y. H. Pei, Q. N. Zheng, and Z. G. Wang, 2012: Modulation of El Niño-southern oscillation by freshwater flux and salinity variability in the tropical Pacific. *Adv. Atmos. Sci.*, **29**, 647–660, doi: 10.1007/s00376-012-1235-4.
- Zheng, F., and J. Zhu, 2010: Coupled assimilation for an intermediate coupled ENSO prediction model. *Ocean Dyn.*, **60**, 1061–1073, doi: 10.1007/s10236-010-0307-1.
- Zheng, F., and R.-H. Zhang, 2012: Effects of interannual salinity variability and freshwater flux forcing on the development of the 2007/08 La Niña event diagnosed from argo and satellite data. *Dyn. Atmos. Oceans*, **57**, 45–57.
- Zheng, F., J. Zhu, R.-H. Zhang, and G.-Q. Zhou, 2006: Ensemble hindcasts of SST anomalies in the tropical Pacific using an intermediate coupled model. *Geophys. Res. Lett.*, **33**, L19604, doi: 10.1029/2006GL026994.
- Zheng, F., J. Zhu, and R.-H. Zhang, 2007: Impact of altimetry data on ENSO ensemble initializations and predictions. *Geophys. Res. Lett.*, **34**, L13611, doi: 10.1029/2007GL030451.
- Zheng, F., J. Zhu, H. Wang, and R.-H. Zhang, 2009: Ensemble hindcasts of ENSO events over the past 120 years using a large number of ensembles. *Adv. Atmos. Sci.*, **26**(2), 359–372, doi: 10.1007/s00376-009-0359-7.